

# OPCPA and new amplification techniques

Hugo Filipe de Almeida Pires

Recent developments in high intensity lasers have allowed increasingly higher powers, up to the Petawatt ( $10^{15}$  W) level. This redefinition of **ultra intense lasers** allows for breakthroughs in several fields of science, by allowing new physics regimes. Among the several laser techniques used to reach these powers, one distinguishes itself drastically due to the several advantages it offers: amplified parametric chirped pulse amplification (OPCPA), based in a three wave mixing process in non-linear crystals. The work shown in this Thesis is framed in GoLP's global initiative to develop an ultra broadband, OPCPA based high energy and repetition rate, with a pump system based in diode lasers. This kind of lasers, in particular associated with ytterbium doped amplifying materials, allows a high efficiency, high repetition rate, operation, therefore being ideal as a pump source for OPCPA. However, the working wavelength for such a system is different from the one used at the laboratory. In this Thesis the experimental work resulting in the full characterization of the current laser system front-end and the current OPCPA chain at wavelengths compatible with a diode based parallel system. Results show it is possible to convert the whole laser chain into an ultra broadband diode pumped system, opening new horizons in the laboratory's laser parameters.

**Keywords and OCIS codes:** 140.0140 Lasers and laser optics, 190.0190 Nonlinear optics, 320.0320 Ultrafast optics, 060.0060 Fiber optics and optical communications

## Introduction

### 1.1. Laser evolution and trends

Lasers, more than ever, are at rapid evolution, with new physics events unlocked for tabletop testing with each new threshold of power and pulse duration attained, allowing for applications in biology, chemistry, plasma physics and fusion among others.

The peak power of a laser pulse is defined as  $P=E/\tau$ , where  $E$  is the energy concentrated in the pulse duration  $\tau$ . Therefore, the growing increase of peak power since the invention of the laser almost fifty years ago has been achieved thanks to a systematic increase in the output pulse energy and a decrease in the shortest pulse duration achievable. However, the conjugation of high energies and short pulses was not feasible, until the introduction of the chirped pulse amplification (CPA) technique in the mid-1980's [1]. This was due to the nonlinear effects experienced by short pulses while travelling inside the optical amplifiers. With CPA, the pulse duration is stretched during amplification and compressed at the end, and such problems are avoided. This was a tremendous turning point in the last 50 years of laser research, as shown in Fig. 1.1. CPA allowed the generation of multi-terawatt pulses in a tabletop fashion, and brought large-scale physics to small-scale laboratories.

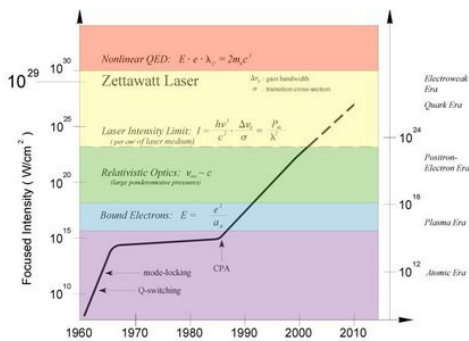


Fig. 1.1 – Laser intensity evolution

### 1.2. Optical parametric chirped pulse amplification

With the increase in power achieved with CPA, intensities were high enough for a whole new class of non-linear phenomena to arise. Newly discovered non-linear crystals  $\beta$ -barium borate (BBO) and lithium triborate (LBO) presented optimal optical characteristics and a high damage threshold, and as such, optical parametric generation (OPG) using these crystals in a CPA setup would allow for frequency flexibility that does not exist in the conventional amplification techniques [2].

The principle of OPG is to take a suitable nonlinear crystal and a high intensity beam (pump beam) and use it to amplify a lower frequency, lower intensity beam (signal beam). Because of energy and momentum conservation, a third beam (idler) is generated at an even lower frequency, such that the sum of the signal and idler frequencies equals that of the pump.

This principle can be used to create an optical parametric oscillator (OPO) or as an optical parametric amplifier (OPA). When OPA is applied to a chirped seed (or signal) in a CPA manner, we speak of **optical parametric chirped pulse amplification** (OPCPA) [3].

Being a nonlinear process high intensities (specially the pump) are required, thus unless an exceptionally small focus is achieved in the crystal a reasonable power is required to begin with. OPCPA is typically used upon pulses with durations from the few fs to the hundreds of picoseconds, from few mJ to the tenths of J per pulse, allowing the generation of output peak powers from the GW to the PW level.

OPCPA has seen ample interest and usage in the scientific community since its development, being the current technique of choice for several European and world scale high intensity laser projects: Vulcan 10 PW at the Rutherford Appleton Laboratory, Petawatt Field Synthesizer at Max-Planck Garching, or Omega EP at Rochester, to name but a few. In retrospective, a clear evolution of both the peak power and pulse duration attained with this technique can be seen, and its comparison with other techniques. In Fig 1.2 one can see how OPCPA has been growing in power and its comparison with solid state amplifiers.

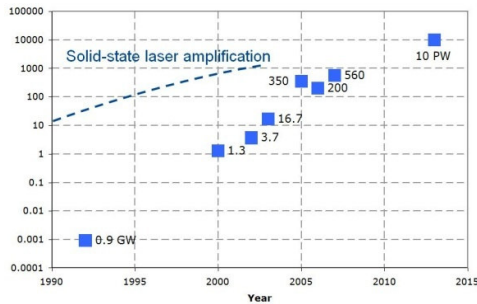


Fig. 1.2 –Evolution of the power of OPCPA based lasers (in TW)

The current popularity of OPCPA is due to a number of significant advantages over traditional amplification based on inverted population. Below is a list of some of the most important ones:

- High gain per single pass, shown up to  $10^5$  [3] which allows improved simplicity and compatibility.
- Low thermal effects thanks to the fact that no population inversion is involved.
- Great wavelength flexibility, limited only by the crystal transparency range.
- No amplified spontaneous emission, which allows for very high contrast .
- Extremely broad amplification bandwidth, allowing ultrashort (few fs) pulses.
- High quantum efficiency which makes for the energy lost to the idler wave.
- High output beam quality.
- Good scalability to high energies.

However, some new drawbacks do exist compared to laser gain media amplification:

- Since there is no pump energy accumulation, the pump must have high intensity.
- Considerable and inevitable losses towards the idler wave.
- High precision pump to signal synchronization needed to achieve good efficiencies.
- Amplified parametric spontaneous emission (in the pump pulse duration window only, making the pump shape also important, top hat being the best).
- Limited aperture of the nonlinear crystals.

### 1.3. Proposed work

The Laboratory for Intense Lasers (L2I) is a facility dedicated to the development and application of high intensity lasers. It hosts a multi-terawatt laser based on CPA in Ti:sapphire and Nd:glass, this being the largest laser system in the laboratory. Additionally, there are two research lines on ultra-broadband OPCPA and diode-pumped, ytterbium-based materials.

OPCPA has been studied by our group since 2004, and this work is framed in a greater goal to **achieve high energy and peak power pulses by using OPCPA pumped by a diode-pumped solid state amplifier (ytterbium-doped amplifying materials).**

The high repetition rate and efficiency of these Yb-based amplifiers makes them ideal to supply the pump for an OPCPA stage. Figure 1.3 shows a schematic of what a diode-pumped OPCPA laser chain looks like: diode lasers are used to pump an Yb-doped amplifier at a high repetition rate, whose output is then frequency doubled and used to pump the nonlinear crystal. Meanwhile, the low energy, chirped seed pulses interact with the pump pulses inside the crystal and are amplified.

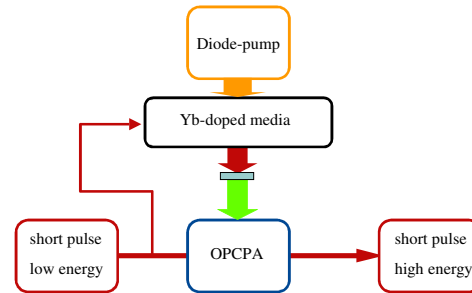


Fig. 1.3 –Schematic of a diode-pumped OPCPA system

In order to be able to operate an OPCPA chain and pump it with an independent, ytterbium-based chain, it is essential to ensure a jitter-free synchronization between the two. The most effective way of achieving this is to use **optical synchronization**: the same laser source is used as a seed for the signal (OPCPA) and pump (ytterbium-based) laser chains. The pulses are split in two, part is sent to the OPCPA crystal, and part is used to seed the Yb-based amplifier (as illustrated in Fig. 1.3). This however requires that the OPCPA process takes place at a wavelength compatible with the operation of the ytterbium-based chain.

At the time when the work described in this Thesis started, a new experimental configuration for ultra broadband amplification with dispersed pulses had been demonstrated at our group [4]. The next steps would be (i) to move to a higher energy pump based on Yb-doped amplification, (ii) to generate an extremely broadband, well characterized signal, and (iii) to study the best wavelength for amplification in this configuration.

In this scenario, the main goal of the work of this Thesis was **the complete characterization of the current front-end of the multi-terawatt laser system, when working at a different wavelength than the standard 1053 nm, compatible with ytterbium-based amplification.** This would require several experimental measurements, adaptation of existing diagnostics, and introduction of new components on the experimental setup. The following list describes the main tasks that were part of this process:

- Completely characterize the performance of the multi-terawatt laser front-end (100 fs oscillator, stretcher and regenerative amplifier) over a range of wavelengths in the near-infrared;
- Develop and apply a picosecond cross-correlator to characterize the wavelength dependence and tunability of a photonic crystal fiber (PCF), used for generating an ultra broadband seed for OPCPA;
- Adapt an existing high-resolution grating spectrometer for ultra broadband operation, capable of dealing with the >200 nm spectra expected;

- Dimension, install and characterize a new frequency doubling crystal for generating the pump pulse, capable of operating in the 1-100 mJ range;
  - Characterize OPCPA at the new wavelengths in the mJ regime.
- In this Chapter we present the facility where the experimental work took place, describe the multi-terawatt laser system and its front-end, and the experimental setup used for our measurements.

## 2.1. Laboratório de Lasers Intensos

We will now look at the experimental facility where this work was developed, by describing the laser chain, and the components relevant to this thesis. Working since 1998, the “Laboratório de Lasers Intensos” has a 10 TW class laser, based on Ti:sapphire and Nd:glass, capable to achieve focused intensities of up to  $10^{19}$  W/cm<sup>2</sup>, making him the most intense laser source in Portugal. Its prime research areas are high power lasers technology, diagnostics, laser-plasma interaction, particle acceleration schemes, X-ray and high harmonic generation.

The lab is inside a 120m<sup>2</sup> class 10.000 clean room, and the general schematic of the 10TW laser is as described in Fig 2.1:

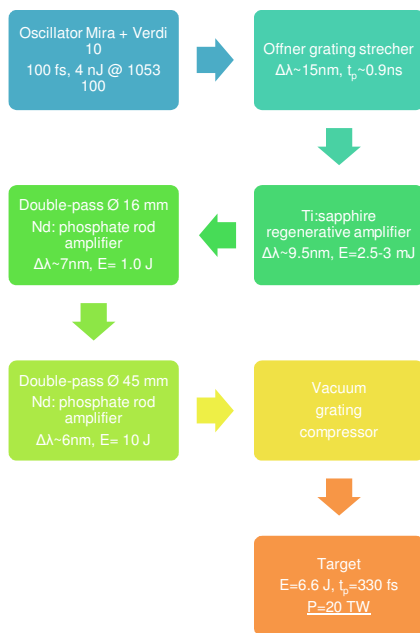


Fig. 2.1 - L2I schematic

### 2.1.1. Oscillator

Our oscillator is a Coherent mode-locked Ti:sapphire laser, model Mira 900-F.

It uses a non standard set of mirrors and is pumped by a 10 W green laser (model Verdi-V10) to achieve mode-locking operation at the wavelength of 1053 nm. Its factory specifications are:

<b>Pulse duration</b>	<130 fs	Assuming sech <sup>2</sup> on a < 200 fs autocorrelation
<b>Repetition rate</b>	76 MHz	Nominal

<b>Noise</b>	<0.1%	Measured rms in a 10Hz to 20 MHz bandwidth
<b>Stability</b>	<3%	Power drift in any two-hour period after warm-up when crystal cooling water is maintained at $\pm 0.1^\circ\text{C}$
<b>Beam Diameter</b>	0.8 mm	$1/e^2$ diameter ( $\pm 0.2\text{mm}$ ) at exit port
<b>Beam Divergence</b>	1.7 mrad	Full angle divergence ( $\pm 0.3$ mrad) at exit port
<b>Spatial Mode</b>	TEM <sub>00</sub>	Typical measured M <sup>2</sup> value is 1.1



Fig. 2.2 - The MIRA 900-F oscillator

The oscillator is tunable by adjustment of a birefringent filter. In order to center its operation at a desired wavelength, a spectrometer is used referenced to the line emission of a Nd:YAG laser.

### 2.1.2. Pulse Stretcher

The stretcher is based on an Offner triplet, with two concentric mirrors providing an aberration free operation in spite of using spherical optics. The gold coated concave and convex mirrors have a surface irregularity than  $\lambda/20$  and  $\lambda/40$  (p-v), respectively.



Fig. 2.3 - The Offner grating stretcher, with the 250 mm diameter concave mirror on the left, convex mirror slab near the center, and diffraction grating pair on the right.

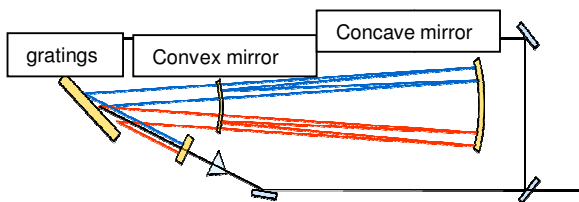


Fig. 2.4 - Diagram of an offner stretcher

The stretcher was dimensioned for a linear dispersion of 60 ps/nm over a 40 nm spectral window ( $2.7 \times \Delta\lambda$  of the current oscillator). However it is currently using a tiled pair of small gratings, slightly clipping the oscillator output. Such limitation will be removed when the small gratings are replaced by a single 120x140 mm<sup>2</sup> one.

### 2.1.3. Regenerative amplifier

The regenerative amplifier is based on a Ti:sapphire crystal pumped by a commercial Nd:YAG laser. In the current configuration it is capable of a net gain of  $>10^7 \times$ , with a typical 3 mJ output energy at 10 Hz and with a contrast ratio of  $10^5$ .



Fig. 2.5 - View of the central part of the regenerative amplifier cavity, showing the Ti:sapphire crystal in the center (on top of a copper mount)

The beam leaving the stretcher feeds the regenerative amplifier which gives around one hundred passes.

At this wavelengths the spectral gain curve of Ti:sapphire is approximately linear, increasing towards shorter wavelengths and, to avoid gain shifting, a polarizer must be present for tuning purposes. The combination of these gain and loss curves plus the finite spectral performance of the optical coatings of the elements within the cavity induce gain narrowing.

The regenerative amplifier is pumped by a Nd:YAG laser from Spectra-Physics, model GCR-130. Its factory specifications are:

	1064	532	
	nm	nm	
Repetition rate	10 Hz		
Output energy	450	200	
	mJ	mJ	
Pulse width	9-12	7-11	FWHM,

ns ns normal mode

## 2.2. Experimental work

Figure 2.6 shows the front-end of the multi-terawatt laser chain that was used for this work. The pulses exiting the oscillator are enlarged and chirped in the stretcher before being amplified – in the case shown, in the Ti:sapphire regenerative amplifier. The compressor, which is not needed for OPCPA, is not shown here.

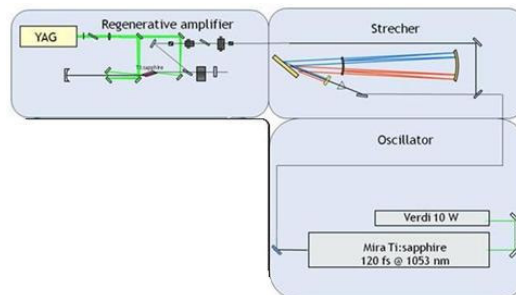


Fig. 2.6 – front-end of the laser chain at L2I

### 2.2.1. Broad energy range crystal

In order to increase OPCPA efficiency a new frequency doubling crystal was modeled using the SNLO software, as shown in Fig. 2.7 [5]. The previously existing crystal was not in any way optimized, and as such, an OPCPA dedicated crystal was in order. The main requirement was a flexible working efficiency in the 1-100mJ range, as to accommodate both pumping from the regenerative amplifier and from Yb doped solid state diode-pumped lasers. Using the software, the choice of the crystal was done by comparing material properties between the “usual” crystals used (LBO, BBO, KDP, DKDP), and by calculating for each the needed dimensions of the crystal, cross-referencing with catalog supply from distributors.

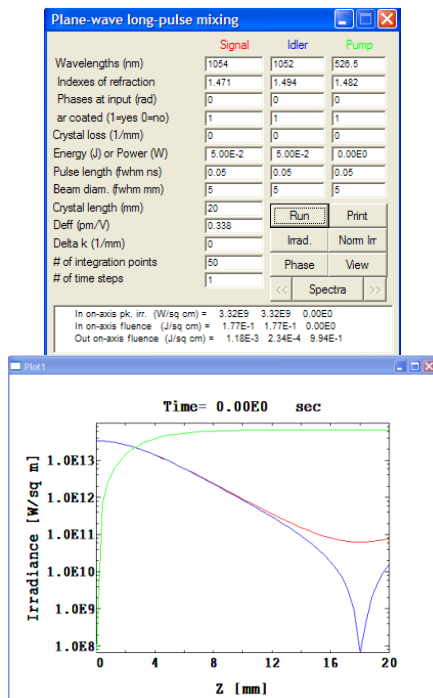


Fig. 2.7 Input parameters and showcase simulation for a 100mJ beam

The decision of purchasing a 12x12 DKDP crystal, due to higher material transparency for the wavelength region of work, was afterwards confirmed by asking the suppliers for their view towards our needs.

The transparency and major physical and optical proprieties are show in the table below and in Fig 2.8.

Chemical formula	$KD_2PO_4$
Hygroscopicity	high
Nonlinear coeff. d36, pm/V at 1054 nm	0.337
Laser damage threshold, GW/cm <sup>2</sup> at 1.06 $\mu$ m	250 ps – 6 ns – 0.5
Density, g/cm <sup>3</sup>	2.355
Thermal conductivity, W/cm $\times$ K	$k_{11} = 1.9 \times 10^{-2}$ $k_{33} = 2.1 \times 10^{-2}$
Thermal expansion coefficients, K-	$a_{11} = 1.9 \times 10^{-5}$ $a_{33} = 4.4 \times 10^{-5}$
Residual absorption, cm-1 (at 1.06 $\mu$ m)	0.005
Measured refractive index (at 1.06 $\mu$ m)	no = 1.4931 ne = 1.4582

## DKDP

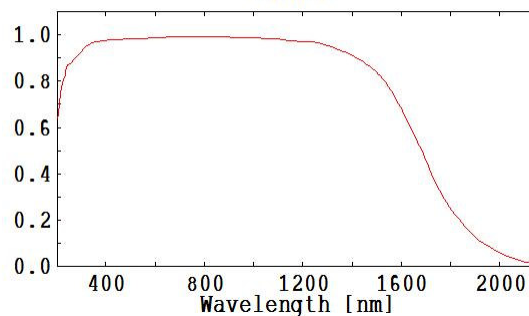


Fig. 2.8 - Transmission through 1cm of DKDP crystal

### 2.2.2. Spectrometer

The commercial spectrometer available at our lab proves to be below what was needed for our characterization, in fact, even with the lowest gratings (150grooves per mm) the total bandwidth seen at a time was of around 100 nm.

The limitation was that although the grating was sufficient, the image was far too large upon reaching the sensor, and as such only half of the width would fit in the CCD.

In order to upgrade the spectrometer to broadband operation, the beam was focused, with a lens, focusing the image into an infrared viewer sensor and relaying the image into the CC camera (thus enabling a greater viewing range as well as extending it to areas where the CCD no longer responded).

The introduction of a lens into the spectrometer (see Fig 2.9) however, may introduce aberrations if any misalignment is present. In order to correct these, and to measure such aberrations several reference beams at different wavelengths were used for calibration and the system was aligned until aberrations were no longer measurable (below the nm scale).

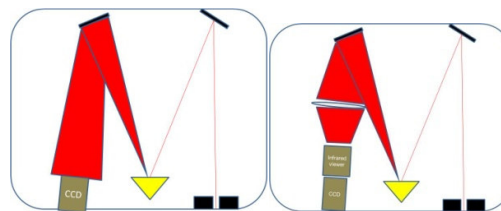


Fig. 2.9 - The oscillator before (left) and after (right) the broadband adaptation

### 2.2.3. Oscillator

Having a broadband spectrometer, the oscillator was tuned to have its central wavelength sweep the 960-1100 nm region, optimizing stability and power at each central wavelength, and measuring the output power with a photodiode as well as recording the spectrum measured with the spectrometer.

### 2.2.4. Photonic crystal fiber

The oscillator output was focused in the fiber entrance, and its output sent to the spectrometer, with the above measures being repeated.

To further characterize the fiber, and to measure its spectro-temporal profile, a self correlation between the fiber output and the oscillator was established as shown in the schematic below. The fiber coil has 5m of length, and as such each pulse exiting the fiber would interact with another pulse different from the first. A delay line was installed to give the same optical path to both arms to ensure optical synchronization. The bandwidth obtained from the fiber was so broadband that the experiment would correlate with only part of it. The phase mismatch angle was therefore varied in each acquisition to ensure full bandwidth was acquired.

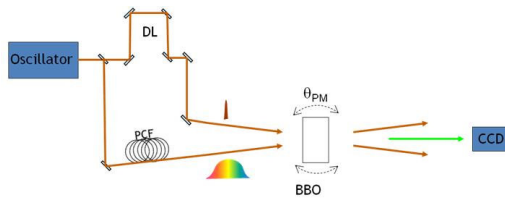


Fig. 2.10 - Correlation setup used for PCF diagnosis

### 2.2.5. Stretcher

A study on the spectral masking of the stretcher was done by carefully placing a mask (paper photographic paper to block the laser pulse) in the convex mirror thus limiting the wavelength window seeding the amplifier.

### 2.2.6. Regenerative amplifier

By tuning a polarizer, a new q-switch wavelength for the cavity was selected, afterwards the input (oscillator) wavelength was varied towards maximizing the exit. The wavelength was of both the oscillator and the exit of the amplifier was then mapped as a function of the q-switch wavelength as well as the output power.

### 2.2.7. OPCPA

The following experimental setup was used to obtain OPCPA:

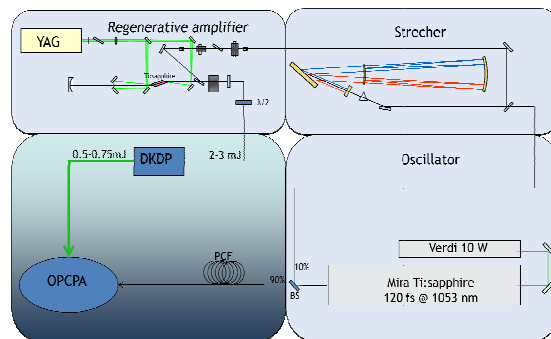


Fig. 2.11 - Experimental setup used for OPCPA

The seed is stretched by traveling through the PCF, and the pump is frequency doubled after exiting the regenerative amplifier using the DKDP crystal. The synchronization is done by selecting the number of laps within the regenerative amplifier and fine tuned by a delay line placed before the PCF fiber (omitted in scheme).

## 3.1. New crystal replacement:

The DKDP crystal was mounted on a specially-designed aluminum frame, and then assembled on a commercial kinematic mirror mount with precision tip and tilt adjustment. The output of the Ti: sapphire regenerative amplifier (~1 mJ, 10 Hz) was focused by a  $f=1$  m convex lens on the crystal, resulting in a  $<200$   $\mu\text{m}$  diameter focal spot. This corresponded to an intensity of approximately  $10$   $\text{GW}/\text{cm}^2$ . The output frequency-doubled pulse was then directed to the BBO crystal by a set of three high-reflective mirrors in the green region, in this fashion eliminating the remaining infrared components. The energy was measured using a power meter. The average conversion efficiency in frequency doubling obtained was 25% ( $25\text{mW} \rightarrow 6\text{mW}$ ), whereas with the previous crystal it was of 10%. In the future, the DKDP crystal will be used with the 100 mJ from the output of the ytterbium-based amplifier.

## 3.2. Oscillator:

The data obtained is shown in Figs 3.1 and 3.2. Measures were limited to the 980-1080 nm range, due to the laser being unable to mode-lock beyond these regions. The increase in power when the laser is made to operate below 1000nm is due to the Ti:sapphire gain curve compensating the loss of reflectivity of the mirrors. Just a little over the limits of the interval, it was possible to operate in mode-lock, by achieving mode-lock within the shown region and to afterwards change the wavelength. This however led not only to an unstable output of power, but occasionally also to the mode-lock lasting only a few minutes.

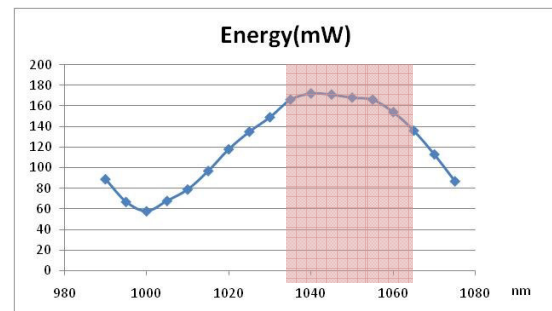


Fig. 3.1 - Average oscillator power

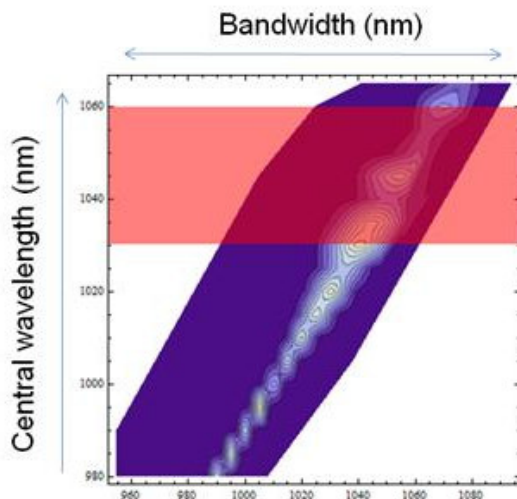


Fig. 3.2 –Oscillator bandwidth study

A maximum energy plateau exists in the 1030-1060nm range with a nearly flat energy variation and increasing bandwidth towards lower wavelengths.

### 3.3. Photonic Crystal Fiber:

Each measurement was done with the central wavelength defined at the oscillator and after oscillator tuning for maximum power. The graph serves as a display of how much bandwidth is available for each central wavelength (set at oscillator). The direct feed into the spectrometer revealed a rather complex and rich pattern. Being a non-linear phenomenon, as expected the broader bandwidths are achieved at wavelengths at which the oscillator has a higher power output. Bandwidths of up to 320nm are visible in the graph.

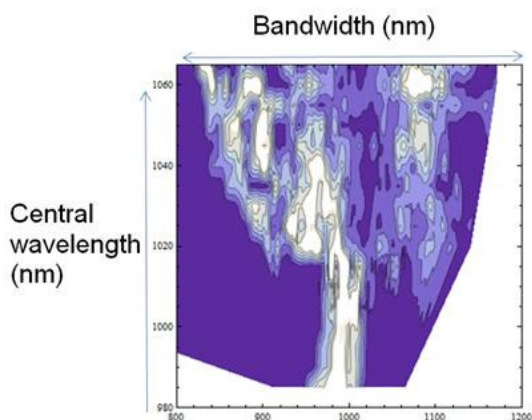


Fig. 3.3 - PCF bandwidth study

From the self-correlation a study of the temporal structure of pulses after passing through the PCF is visible, and a clear parabola but, of complex intensity distribution, shows that a pulse stretched by the fiber will not be compressible.

Each acquisition (horizontal line) was done with different filters as to prevent saturation but have as much resolution as possible. The first graph shows the data as acquired, and the second one

had each line normalized accordingly with the filter used to display the right intensity relation.

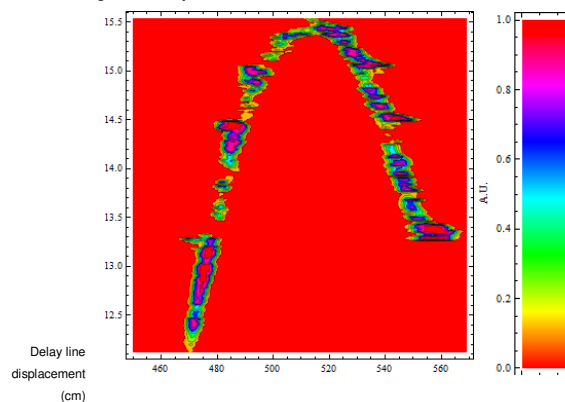


Fig. 3.4 - unnormalized spectro-temporal profile

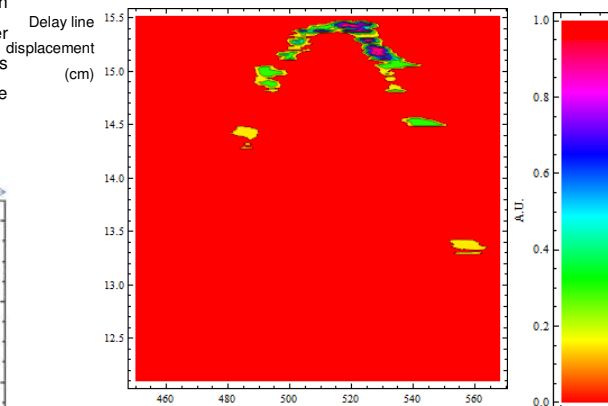
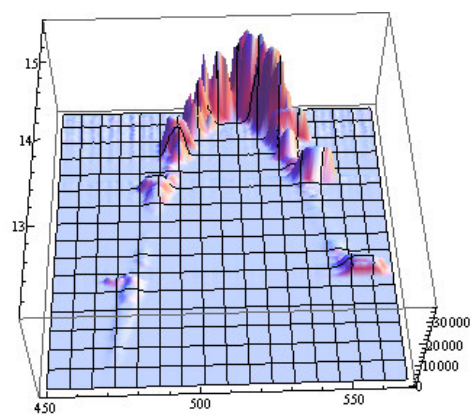


Fig. 3.5 PCF spectro-temporal profile

### 3.4. Spectral masking of the pulse in the stretcher

Due to the sensitivity of the mirror where the masking was done, a quantitative measure on the window left unclipped was not possible to arrange, the pragmatic way found to deal with this predicament was to determine the positions on each edge of the mirror where the masking began to have effects, and to keep one the filters in place and to successively move the other more. The horizontal coordinate is therefore the number of the measure. As the horizontal coordinate increases more and more spectrum of the

seed is being clipped. The two sets of data represent which wavelengths are being filtered out.

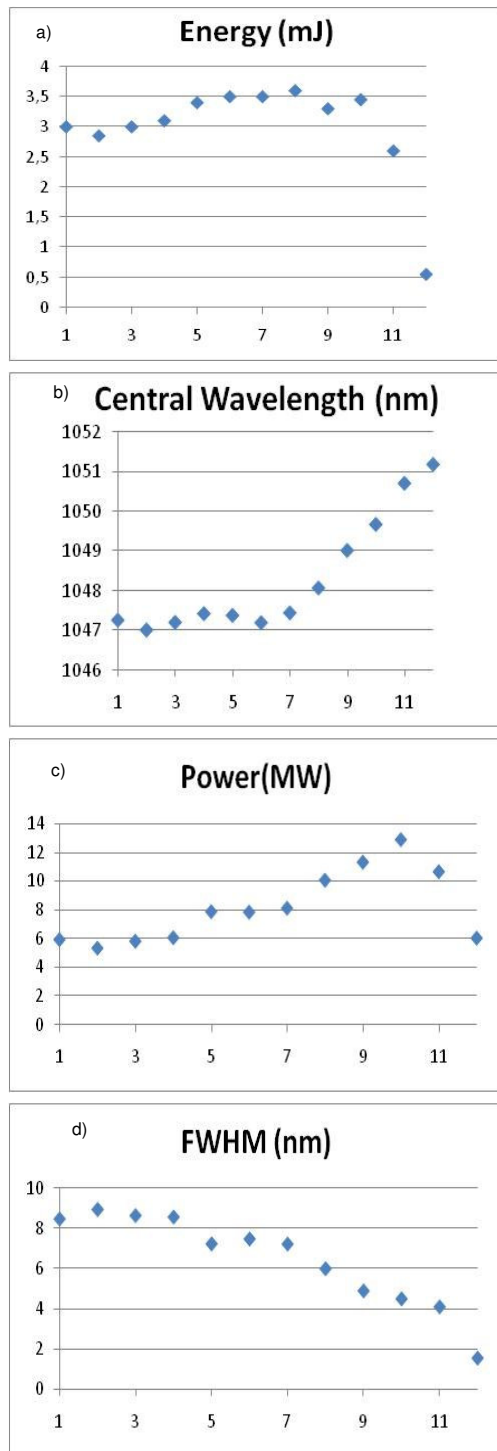


Fig. 3.6 – masking effect when clipping shorter wavelengths. a) The energy of the output of the regenerative amplifier b) Central wavelength of the output of the regenerative amplifier c) Power of the output of the regenerative amplifier d) Bandwidth (full width at half maximum) of the output of the regenerative amplifier

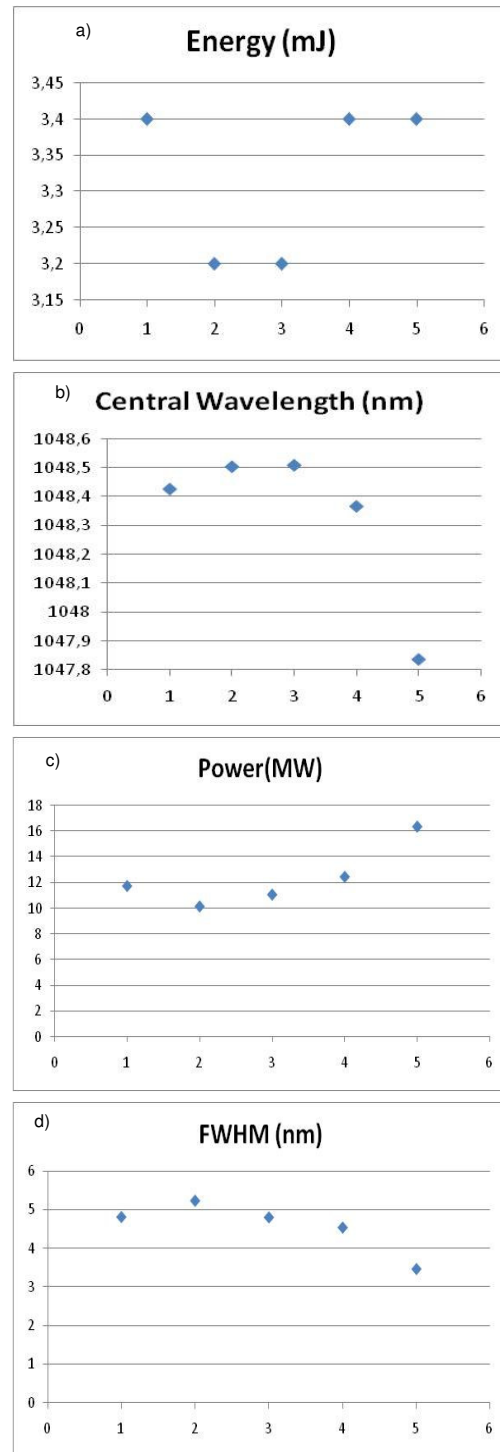


Fig. 3.7 - masking effect when clipping longer wavelengths. a) The energy of the output of the regenerative amplifier b) Central wavelength of the output of the regenerative amplifier c) Power of the output of the regenerative amplifier d) Bandwidth (full width at half maximum) of the output of the regenerative amplifier

The data shows that a slight increase in power is obtainable by slightly trimming both edges of the oscillator spectrum. This is due to the oscillator having a bandwidth that can be fully amplified by the regen amplifier but that cannot be extracted. Thus energy of the Ti:sapphire is being spent amplifying wavelengths being blocked

by the polarizer responsible for the extraction of energy from the cavity.

### 3.5. Regenerative amplifier tunability:

Both the oscillator and the Ti:sapphire regenerative amplifier can be continuously tuned between 1030 and 1055 nm. The operating wavelength of the amplifier is mostly set by the intra cavity polarizer and the spectral response of the cavity optics. The horizontal axis displays the q-switch wavelength (the wave length defined by the intra cavity polarizer). And for each defined q-switch wavelength, the oscillator was optimized and its central wavelength recorded (green markers), as well as the central wavelength of the regenerative amplifier output (red markers).

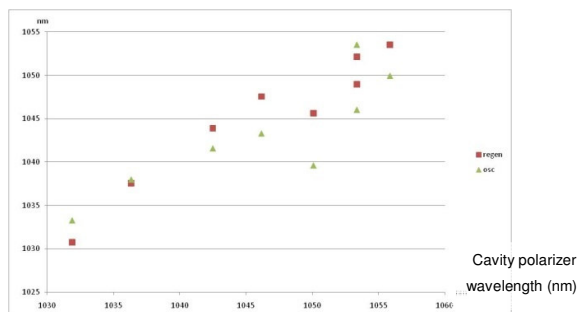


Fig. 3.8 - Regenerative amplifier tunability

For each measurement the output power of the regenerative amplifier was also measured with a photodiode, and showed only a 10% variation of maximum, which indicates flexibility.

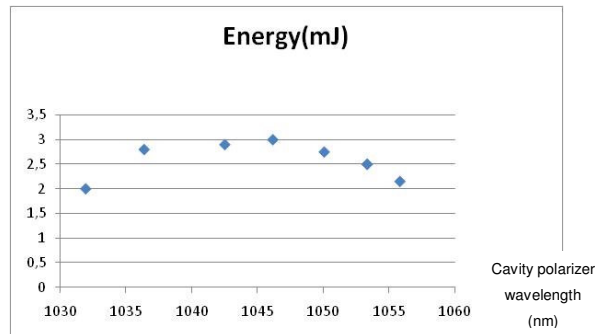


Fig. 3.9 – Regenerative amplifier output power as a function of the q-switch wavelength

### 3.6. Experimental verification of OPCPA

With the regenerative amplifier and the oscillator both tuned at 1045 nm, a wavelength chosen after analyzing the data displayed above, for which the regenerative amplifier and the oscillator output powers are maximized, OPCPA was achieved. The signal power was of 170mW, and the energy of the pump was 0.7mJ. With the increase in energy from the pump up to  $10^6$  amplification was expected but a nonlinear parasitic phenomenon was present and dominated the interaction (OPCPA was impossible to observe beneath it). The pump was then filtered (using neutral density filters) and OPCPA became visible as the previous phenomenon disappeared, the measured amplification was of  $10^{1.6}$  explained

from the fact that the phenomenon is non-linear. Data acquired was not required for another lab incursion was planned to take place where more satisfactory data would be acquired, unfortunately and due to technical problems this day was delayed. However, and since previous OPCPA experiments have been done by our group with the same pump, the changes are only the new frequency doubling crystal and a wavelength shift from the 1054nm to the 1045nm. Therefore and considering the global picture this result is of very little importance. And having successfully study the tenability of our front-end the next experimental incursion would be to obtain OPCPA with the Yb-based amplifiers.

### Conclusions

We have demonstrated that the front-end can be operated in the 1030-1060 nm range with output power 2-3 mJ, and that by using a spectral mask up to another 0.5mJ can be added with minimal spectral content loss (around 11%), by clipping mostly unextractable wavelengths.

The characterization of the pulses allows accessing optimum working wavelengths for any experiment that uses the front-end and possesses some wavelength flexibility.

The spectrometer upgrade turned out to be able to supply the needed analysis, and should help in future ultra-broadband experiments. The use of a PCF for generating an ultra broadband pulse proved to be an easy and tunable way to obtain bandwidths of several hundreds of nm. The spectral widening is highly dependent on the intensity of the beam crossing the fiber, in such a manner that by slightly reducing the seed power (or by slightly misaligning the entrance to the fiber) the amount of bandwidth can be selected. The picosecond self-correlation shows that  $2^{\text{nd}}$  order distortions are introduced, making a pulse stretched by such a PCF impossible to be restored to its original duration of the usual compressors.

In the regent amplifier OPCPA results were below expected due to the arise of an initially not understood non-linear noise phenomenon. Thought to be amplified parametric spontaneous emission at first, after calculations and comparison to previous OPCPA experiments done at L2I, it became apparent that over-caution was to blame as the pump was not sufficiently focused for the amplification to be the dominant event. Further attempts were impossible to perform once again due to the technical setback at the laboratory.

As a whole, results were satisfactory in the manner that the characterization of the laser chain was of vital importance. Regretfully, due to a technical malfunction in the air conditioning system of the laboratory, the final stage of replacing the regent amplifier by the solid state laser amplifier was not done as of this point. However, the work done in this Thesis allows for a prior wavelength selection of such a laser chain by cross-referencing the data here shown with data recently obtained in a parallel work of diagnosing such amplifier.

This work has succeeded in laying all necessary foundations towards building an OPCPA chain pumped by solid state Yb:doped amplifiers. Having done this work, the next step is to replace the pump amplification stage from the regenerative amplifier to the solid state one. Having an increase of energy from the 3mJ of the regent to the 30-100mJ of the Yb:doped materials, should allow for

high amplification at a high repetition rate (since heat deposition is expected to be minimal).

## References

- [1] [2] Giulio Cerullo and Sandro De Silvestri, "Ultrafast optical parametric amplifiers", *Rev. Sci. Instrum.* 74, (2003)
- [3] I. N. Ross *et al.*, "The prospects for ultrashort pulse duration and ultrahigh intensity using optical parametric chirped pulse amplifiers", *Opt. Commun.* 144, 125 (1997)
- [4] L. Cardoso, "Experimental results on ultra-broadband OPCPA" oral presentation, CLEO Europe 2007
- [5]<http://www.as-photonics.com/SNLO/>